Rev. Mexicana Astron. Astrof., **23**, 223-230 (1992)

HYDROGEN OPACITIES AT HIGH DENSITIES

Paolo Lenzuni
Center for Radiophysics and Space Sciences
Cornell University
and
Didier Saumon
Lunar and Planetary Laboratory
University of Arizona

RESUMEN. Discutimos las opacidades del continuo en un gas de hidrógeno de alta densidad ($\rho \geq 10^{-3}$ g cm^{-3}), haciendo especial énfasis en la absorción por H_2 inducida por colisiones y la fotoseparación de H^-.

ABSTRACT. We discuss continuum opacities in a high-density ($\rho \geq 10^{-3}$ g cm^{-3}) hydrogen gas, with special emphasis on collision-induced absorption by H_2 and photodetachment of H^-.

Key words: OPACITIES – STARS: LOW-MASS

I. INTRODUCTION

Models of dense stellar atmospheres have long been recognized to suffer from several over simplifications. One of the most crucial is the use of atmospheric opacities that have been calculated assuming that the various species in the gas mix ideally and ignoring all non-ideal effects (for a recent and extensive calculation see Lenzuni, Chernoff, & Salpeter 1991). In addition, models of collision-induced absorption (CIA) by H_2-H_2 complexes, which dominates the opacity at low temperatures, are still somewhat incomplete, and in particular no calculation has ever been performed to incorporate the effect of multi-body collisions. In this paper we present a first attempt to extend our knowledge of the optical properties of a pure hydrogen fluid to the regime of very high densities ($10^{-3} \leq \rho \leq 0.5$ g cm^{-3}).

There are two distinct astrophysical environments in which our results are expected to be important. Population II and (hypothetical) Population III stars of very low mass have very dense atmospheres whose modeling requires the use of reliable opacities for a dense molecular fluid. Similarly, models of old white dwarfs, where gravitational settling has operated to leave behind a hydrogen-rich atmosphere, need an improved understanding of opacities in a dense partially ionized plasma.

II. LOW-TEMPERATURE OPACITY

At high densities and low temperatures ($T < 4000$ K), hydrogen is almost completely molecular. In this regime opacity is largely due to collision-induced absorption by H_2-H_2 complexes for frequencies $\nu < \nu_1$, with ν_1 ranging from 13000 cm^{-1} (at $\rho = 0.01$ g cm^{-3}) to 20000 cm^{-1} (at $\rho = 0.5$ g cm^{-3}) (Lenzuni, Chernoff & Salpeter 1991). At frequencies $\nu > \nu_1$ opacity is instead contributed mostly by Rayleigh scattering by H_2. The peak of the Rosseland mean weighting function occurs at frequencies $\nu \leq 15000$ cm^{-1}, so that opacity means are dominated by CIA.

The frequency-integrated CIA has long been known to admit an expansion in powers of the density

$$\kappa = \kappa_1 \rho + \kappa_2 \rho^2 + \kappa_3 \rho^3 + \ldots \tag{1}$$

(Van Kranendonk 1957, 1959). It has been recently shown (Moraldi 1991) that spectral functions (i.e. the monochromatic spectra) also admit a similar expansion. The coefficient κ_1 is a property of the isolated molecule and vanishes for H_2 which is homonuclear. The coefficients κ_2, κ_3, ... are called binary, ternary, ... absorption coefficients and can be related to two-, three-, ...-body processes. In the low-density limit, CIA is described by the binary theory (Meyer, Frommhold & Birnbaum 1989), which has proved very successful in reproducing the spectra observed in laboratory experiments at room temperature. Analytical representations of the line profiles exist, which can be employed at the higher temperatures of astrophysical interest (see Lenzuni, Chernoff & Salpeter 1991 and references therein).

For increasingly large densities, terms of higher and higher order in equation (1) become important. The ratio κ_3/κ_2 has been measured experimentally for H_2-H_2 at room temperature by Hare and Welsh (1958), who find

$$\frac{\kappa_3}{\kappa_2} = 4.5 \times 10^{-4} \quad \text{amagat}^{-1}. \tag{2}$$

Three-body collisions are expected to play an important role for densities $\rho > 200$ amagat (about 0.02 g cm^{-3}) and dominate above 2000 amagat. No measurements are available to estimate the size of κ_4 for CIA by H_2-H_2 complexes. The ratio κ_4/κ_3 has been measured for H_2-He by Dossou, Clermontel & Vu (1986), who find

$$\frac{\kappa_4}{\kappa_3} = 10^{-4} \quad \text{amagat}^{-1} \, . \tag{2b}$$

Based on this measurement, we assume that in a pure hydrogen plasma, n-body collisions with $n > 3$ are never dominant. In the following we shall limit our analysis to binary and ternary spectra, ignoring terms of higher order.

The coefficient κ_3 has been shown by Van Kranendonk (1959) to consist of the sum of three terms

$$\kappa_3 = \kappa_{31} + \kappa_{32} + \kappa_{33}. \tag{3}$$

Here the term κ_{31} describes finite volume effects, κ_{32} results from a negative interference between the dipoles induced in the complex of three interacting molecules, and κ_{33} is concerned with the non-additive part of the induced moment. Recalling that finite volume effects are the single largest non-ideal contribution to the gas pressure of a high-density molecular gas (c.f. Fontaine, Graboske & Van Horn 1977; Magni & Mazzitelli 1979; Saumon 1989), we estimate κ_{31} from the equation

$$\kappa_{31} \rho = \kappa_2 \left(\frac{P}{P_{\rm Th}} - 1 \right), \tag{4}$$

where P and $P_{\rm Th}$ are the total and ideal (thermal) pressure respectively. Pressure is calculated using the non-ideal equation of state (EOS) of Marley & Hubbard (1988). Our assumption can be checked as follows: from Van Kranendonk (1959) we estimate

$$\kappa_{31} = \frac{5}{4} |\kappa_{32}| \tag{5}$$

(see his Table II), and assume that κ_{33} can be ignored. Then we have

$$\kappa_3 \simeq \kappa_{31} + \kappa_{32} = \frac{1}{5} \kappa_{31}. \tag{6}$$

The available experimental results for κ_3 (Chisholm & Welsh 1954; Hare & Welsh 1958) can then be compared with our estimate of κ_{31} from eq. (4), and we find very good agreement. Note that since P comes from a Monte Carlo simulation of multi-body interactions, finite-volume effects are accounted for exactly. Indeed equation (4) should be more properly written as

$$\sum_{n=3} \kappa_{n1} \rho^{n-2} = \kappa_2 \left(\frac{P}{P_{\rm Th}} - 1 \right) \tag{7}$$

which shows explicitly that we calculate finite-volume effects not only in the ternary absorption coefficient but in all the higher expansion terms as well. Finite-volume effects act only on the frequency of collisions but do not alter the details of the collision itself. Since the shape of CIA does not depend on the frequency of collisions, these effects simply scale the low-density binary spectrum by a frequency-independent factor.

The negative contribution associated with the term κ_{32} is known to consist of a series of narrow dips in the absorption spectrum, each centered at the frequency of a roto-vibrational transition of the H_2 molecule (Van Kranendonk 1957). These dips are caused by inter-collisional interference effects in which the dipoles induced in successive collisions tend to cancel each other. At room temperature the dip at the frequency of the $Q(1)$ line (4155.25 cm^{-1}) is by far the most important, and has been modeled by Bouanich et al. (1990) with a Lorentzian line shape whose width scales linearly with ρ. Nothing is known about the temperature dependence of these dips; at the much higher temperatures of astrophysical interest the superposition of the broadened line shapes associated with each transition should presumably wash out all the narrow features of the spectrum. We have ignored this term in our Rosseland mean calculation based on two additional facts: 1) the (negative) absorption is strongest at the line center where the opacity is largest and contributions to κ_R smallest; and 2) opacity at the highest densities is dominated by absorption in double (and possibly triple) transitions, which are unaffected by the cancellation effect.

Very little is known about the spectrum produced by the non-additive part of the dipole induced in clusters of three molecules. Using our model of finite volume effects, we find evidence in the laboratory spectra of Hare & Welsh (1958) that the effect of the non-additive dipole is most significant far from the center of the fundamental band ω_0, and it grows with the distance from ω_0. In a three-body collision, triple transitions can be excited which contribute to the absorption spectrum at frequencies further from the band center than the single and double transitions possible in binary collisions. This might explain the enhanced absorption in the far wings of the fundamental band detectable in the spectra of Hare and Welsh. In terms of integrated absorption, this appears to be a minor contribution, which validates *a posteriori* the assumption made in writing equation (6). We give a very coarse treatment of this contribution by assuming that the induced dipole is identical to that induced in binary collisions, and using a total kinetic energy of the reactants which takes into account the presence of three particles.

In Figure 1 we show the binary and ternary spectra of CIA by H_2-H_2 complexes and the total monochromatic opacity at two different densities. At densities lower than about 0.1 g cm^{-3} opacity is mostly contributed by binary processes. The contribution from multi-body effects is large only at the highest frequencies. However since opacity is lowest precisely at those frequencies, where the weighting function is also large, their inclusion alters the Rosseland mean (κ_R) appreciably. Above 0.1 g cm^{-3} multi-body effects dominate, and κ_R shows large departures from the values predicted by the binary theory.

It is important to keep in mind, however, that our understanding of the entire spectral region longward of the fundamental band, including the region where the transition between CIA and Rayleigh Scattering takes place, is still rather sketchy. The understanding and evaluation of the opacities in this region is crucial to an accurate determination of the Rosseland mean opacity, especially for temperatures $3000 < T < 4000$ K, where the gas is still predominantly molecular and the weighting function has its maximum in this frequency range ($12000 < \nu < 19000$ cm^{-1}). Algorithms appropriate for high-temperature binary spectra exist for the purely rotational and the fundamental vibrational band, but there are no published models for the overtone and hot bands. These bands fall in spectral regions which are otherwise very transparent, and to which the Rosseland mean is therefore very sensitive. Indeed they have been shown in the case of H_2-He CIA to produce very large changes (Lenzuni, Chernoff & Salpeter 1991). On top of these uncertainties in the binary spectrum, falls the existence of unknown but possibly substantial contributions from multi-body contributions discussed in this work, in particular those associated with the coefficient κ_{33}. Finally it is important to note that all the mechanisms that we ignore provide positive contributions to the opacity, and that therefore with our present results we are certainly underestimating the real opacity of the gas in this regime.

III. HIGH-TEMPERATURE OPACITY

For temperatures $4000 < T < 10000$ K a high-density hydrogen gas is in a state of weak ionization, and opacity is dominated by bound-free and free-free processes in H^-. Therefore, in order to give a reliable estimate of the opacity in this regime, it is essential to calculate accurately the ionization equilibrium and the densities of

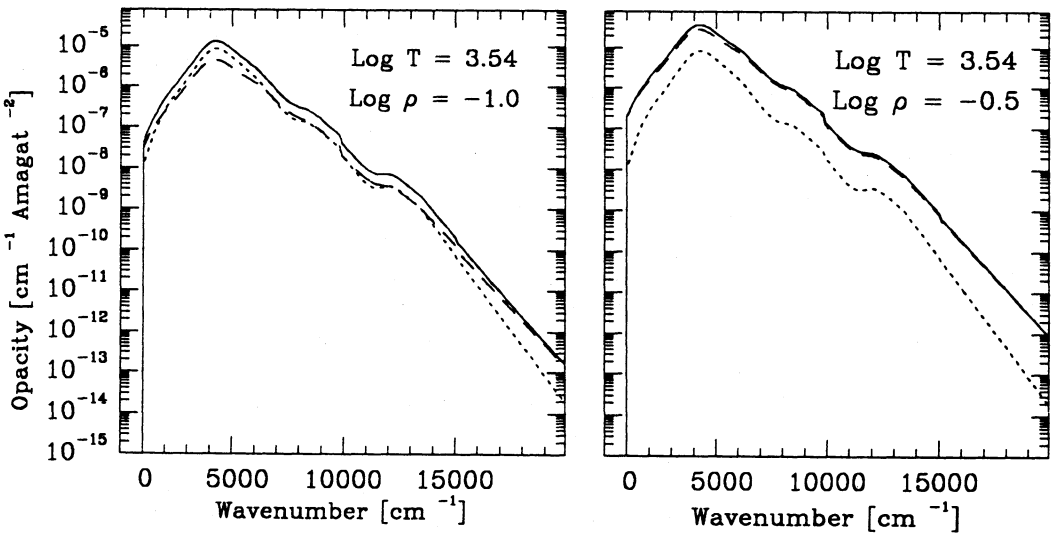

Fig. 1. Collision-induced absorption by H_2 for $\log\rho = -1.0$ and -0.5g cm^{-3}, with $\log T = 3.54$. Shown are the absorption produced by two-body processes (dotted lines), by three-body processes (dashed lines), and the total absorption (solid lines).

all the charged species in the gas. We have used for this purpose a version of Saumon and Chabrier's (1989, 1991) equation of state, modified to include the trace species H^-, H_2^+, H_3^+. The work of Saumon & Chabrier represents the latest effort to describe the thermodynamics of a fully non-ideal mixture of H_2, H, H^+, and electrons where the chemical equilibrium state of the system is determined self-consistently with the non-ideal interactions.

Because the abundances of H^-, H_2^+, and H_3^+ are small under the conditions of interest, they can be introduced in Saumon and Chabrier's EOS by a perturbation treatment. Since it is not practical to recompute the chemical equilibrium of the new set of species with the model of Saumon and Chabrier, this perturbation treatment is based on the assumption that the trace species mix nearly ideally, and therefore uses the Saha equation of ionization and dissociation. Slight non-ideal effects are brought in these equations by introducing a density dependence in the internal partition functions and in the binding energies. Two different kinds of interparticle interactions must be included in the treatment of a dense, partially ionized fluid.

1) The so-called excluded volume interaction, which arises from the finite size of particles with bound states. This includes all species but electrons and H^+. The finite size of the particles effectively reduces the spatial extent of the wavefunctions of bound states and contributes to the removal of states in the internal partition function sum. We treat this interaction within the occupation probability formalism of Hummer and Mihalas (1988). This formalism introduces a smooth state-by-state cutoff in the sum which is consistent with the interparticle interactions. The excluded volume interaction is characterized by the hard sphere diameters σ of the species present. Table 1 gives the values which we have adopted. For H and H_2, the diameters are extracted from the EOS calculation of Saumon and Chabrier (1991) and have a temperature and density dependence which derives from a thermodynamic criterion. The values for H^-, H_2^+, and H_3^+ are estimated from the spatial extent of the electronic wave functions of each state. References for the wavefunctions and internal states of these species are given in Table 1, along with the ionization/dissociation energies of the unperturbed ground states E_B.

2) At the large densities that we investigate, the number density of charges is always substantial for $T \geq 5000$ K. In this kind of environment perturbations are mutually induced in the structures of all the charged species. Because of its small binding energy, the H^- ion is especially sensitive to external perturbations. The other charged particles with bound states (H_2^+, H_3^+) have much larger ionization potentials and are relatively unaffected. We ignore structural changes in these two ions induced by Coulomb interactions. For the perturbed structure of the H^- ion, we apply the results of Yukhnovskii (1988) who has solved the Hamiltonians of H and H^- with electron-electron and ion-electron Coulomb potentials screened by the surrounding plasma. While Yukhnovskii uses the Thomas-Fermi screening length, which is appropriate for a plasma of degenerate

TABLE 1. Atomic Parameters

Ion	$\sigma(\AA)$	E_B (eV)	references
H_2	1.63 - 2.20	4.478	Saumon & Chabrier 1991
H	1.36 - 1.78	13.598	Saumon & Chabrier 1991
H^-	2.3	0.755	Pekeris 1962
H_2^+	2.64	2.651	Huber & Herzberg 1979, Saumon & Chabrier 1991
H_3^+	1.3	4.354	Chandra et al. 1991

electrons, his results can be readily applied to our lower density conditions by substituting the Debye screening length in the expression of the screened Coulomb potential. Yukhnovskii tabulates the binding energies of H and H^- as a function of the screening length, i.e. of the charge density. Because the screened potential used in the Hamiltonian is weaker than the pure Coulomb potential, the binding energies decrease with increasing charge density. The detachment energy of H^- relative to $H + e^-$ also decreases with increasing charge density, but it remains positive even for small values of the screening parameter, in contradiction with the results of Tarafdar & Vardya (1970). In Figures 2a and 2b we compare the abundances of the various species that we calculate in this work, with the abundances given by an ideal equation of state for $\log T = 3.54$. While $n(H_2)$ is always essentially identical in the two cases, $n(H_3^+)$, $n(H^-)$ and $n(e^-)$ at the highest densities are all larger in the non-ideal case. In particular the larger abundance of H^- obtained with the non-ideal EOS is mostly due to simultaneous larger abundances of both neutral hydrogen **and** electrons. The analogous comparison for $\log T = 4.02$ (Figures 2c and 2d) shows that the sign of the effect is now reversed: because of the small occupation probability of its only bound state due to the large excluded volume effects, the non-ideal abundance of H^- is smaller than its ideal counterpart.

Opacity in this regime is mostly contributed by the photodetachment of H^-,

$$H^- + h\nu \rightarrow H + e^- \ , \tag{8}$$

and by free-free absorption by H^-

$$H + e^- + h\nu \rightarrow H + e^- . \tag{9}$$

To zeroth order, the free-free process (9) does not depend on the structure of the H atom, and the corresponding opacity coefficient can be taken from the literature. Conversely, the photodetachment cross section of H^-, $\sigma_\nu(H^-)$, must be reevaluated taking into proper account the structural changes which take place in this ion. In this work we only include the effects due to changes in the binding energy. We use the functional form for the unperturbed $\sigma_\nu(H^-)$ given by John (1988), and substitute the actual value of the binding energy calculated as described above in the place of the the binding energy of the isolated ion. The resulting cross sections are shown and compared in Figure 3 with the analogous quantity for the isolated ion. In a more rigorous treatment of this process one should recalculate $\sigma_\nu(H^-)$ using the wavefunction appropriate for each value of the screening length. Results obtained using this procedure will be published in a forthcoming paper (Lenzuni et al. 1992).

IV. RESULTS AND CONSEQUENCES FOR STELLAR ATMOSPHERES

In Table 2 we compare our present results for the Rosseland mean opacity κ_R with those obtained from a model which ignores non-ideal effects and includes only a binary theory of CIA, labeled as $(\kappa_R)^*$. At the low temperatures at which absorption is dominated by collision-induced processes in H_2, the inclusion of three-body effects results in very substantial increases in the values of the Rosseland mean. The effect is largest at the highest densities, where opacity is indeed mostly contributed by processes associated with multi-body collisions. While opacity in Population I as well as in Population II stars is dominated by metals, the optical properties of zero-metallicity stars are dominated by hydrogen, with helium providing only a moderate contribution.

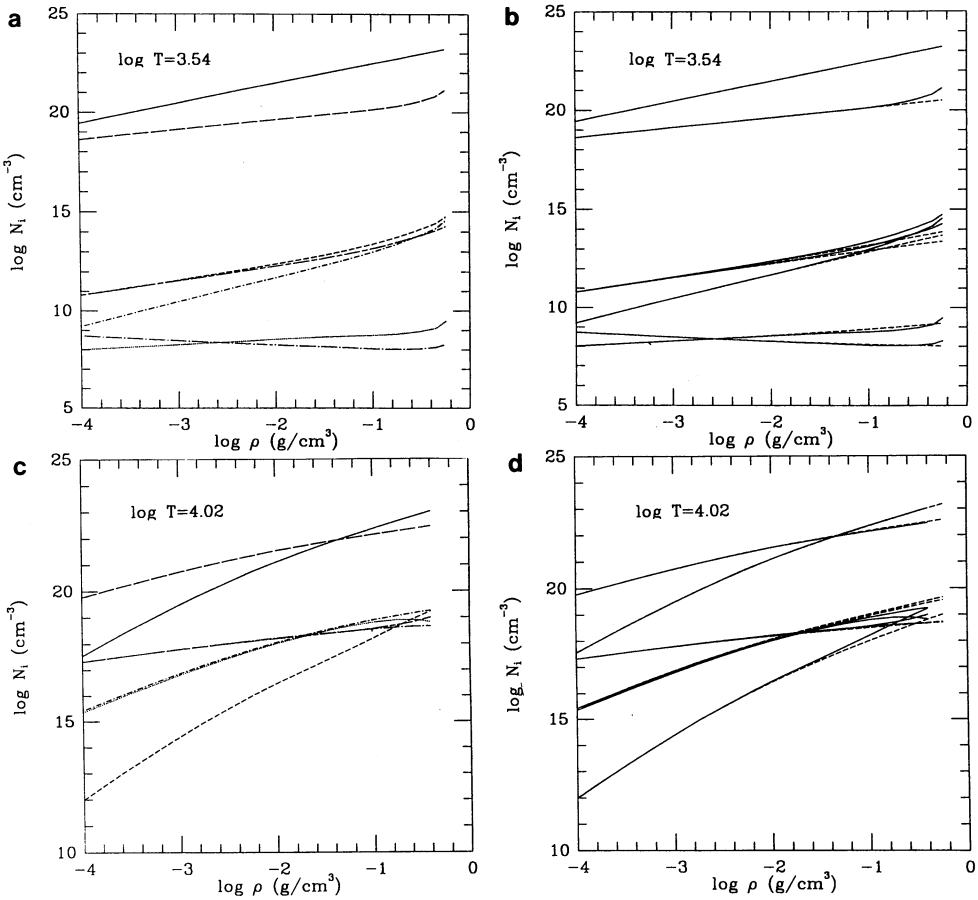

Fig. 2. (a) Non-ideal abundances for $\log T = 3.54$. Shown are the abundances of H_2 (solid line), H_2^+ (dot), H_3^+ (short dash), H (long dash), H^- (short dash-dot), H^+ (long dash-dot), e^- (short dash-long-dash). (b) Non-ideal abundances as in (a) (solid lines) compared to ideal-gas abundances (dashed lines). (c) and (d): the same as in (a) and (b) for $\log T = 4.02$.

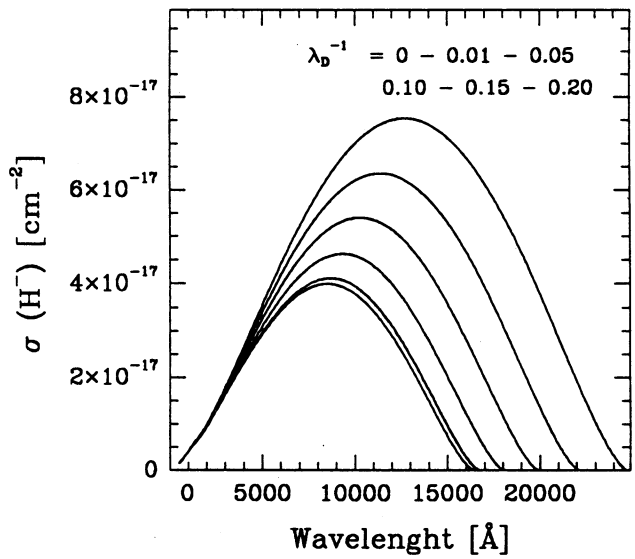

Fig. 3. H^- photodetachment cross section for six different values of λ_D^{-1} in the range 0–0.20.

TABLE 2. Rosseland Mean Opacities

$\log\rho$	$\log T$	κ_R	$(\kappa_R)^*$	$\log\rho$	$\log T$	κ_R	$(\kappa_R)^*$
−3.0	3.38	9.14×10^{-4}	9.14×10^{-4}	−2.5	3.38	1.53×10^{-3}	1.53×10^{-3}
−3.0	3.46	6.85×10^{-4}	6.87×10^{-4}	−2.5	3.46	1.05×10^{-3}	1.05×10^{-3}
−3.0	3.54	2.82×10^{-3}	2.92×10^{-3}	−2.5	3.54	4.32×10^{-3}	4.46×10^{-3}
−3.0	3.62	5.01×10^{-2}	5.32×10^{-2}	−2.5	3.62	7.41×10^{-2}	7.83×10^{-2}
−3.0	3.70	6.85×10^{-1}	7.35×10^{-1}	−2.5	3.70	9.65×10^{-1}	1.04×10^{0}
−3.0	3.78	8.37×10^{0}	9.00×10^{0}	−2.5	3.78	9.58×10^{0}	1.05×10^{1}
−3.0	3.86	7.86×10^{1}	8.58×10^{1}	−2.5	3.86	8.57×10^{1}	9.67×10^{1}
−3.0	3.94	4.27×10^{2}	4.74×10^{2}	−2.5	3.94	5.24×10^{2}	6.13×10^{2}
−3.0	4.02	1.46×10^{3}	1.68×10^{3}	−2.5	4.02	2.03×10^{3}	2.47×10^{3}
−3.0	4.10	3.58×10^{3}	4.47×10^{3}	−2.5	4.10	5.47×10^{3}	7.05×10^{3}
−2.0	3.38	2.38×10^{-3}	2.35×10^{-3}	−1.5	3.38	3.66×10^{-3}	3.39×10^{-3}
−2.0	3.46	1.56×10^{-3}	1.54×10^{-3}	−1.5	3.46	2.38×10^{-3}	2.22×10^{-3}
−2.0	3.54	6.90×10^{-3}	7.00×10^{-3}	−1.5	3.54	1.20×10^{-2}	1.13×10^{-2}
−2.0	3.62	1.10×10^{-1}	1.14×10^{-1}	−1.5	3.62	1.73×10^{-1}	1.67×10^{-1}
−2.0	3.70	1.36×10^{0}	1.45×10^{0}	−1.5	3.70	1.99×10^{0}	2.00×10^{0}
−2.0	3.78	1.17×10^{1}	1.28×10^{1}	−1.5	3.78	1.53×10^{1}	1.62×10^{1}
−2.0	3.86	8.81×10^{1}	1.02×10^{2}	−1.5	3.86	9.36×10^{1}	1.09×10^{2}
−2.0	3.94	5.49×10^{2}	6.84×10^{2}	−1.5	3.94	5.24×10^{2}	6.94×10^{2}
−2.0	4.02	2.34×10^{3}	3.13×10^{3}	−1.5	4.02	2.27×10^{3}	3.40×10^{3}
−2.0	4.10	7.08×10^{3}	1.02×10^{4}	−1.5	4.10	7.48×10^{3}	1.26×10^{4}
−1.0	3.38	6.82×10^{-3}	4.72×10^{-3}	−0.5	3.38	1.68×10^{-2}	6.48×10^{-3}
−1.0	3.46	4.55×10^{-3}	3.22×10^{-3}	−0.5	3.46	1.43×10^{-2}	4.92×10^{-3}
−1.0	3.54	2.73×10^{-2}	1.88×10^{-2}	−0.5	3.54	1.11×10^{-1}	3.43×10^{-2}
−1.0	3.62	3.43×10^{-1}	2.52×10^{-1}	−0.5	3.62	1.18×10^{0}	4.23×10^{-1}
−1.0	3.70	3.51×10^{0}	2.78×10^{0}	−0.5	3.70	1.01×10^{1}	4.34×10^{0}
−1.0	3.78	2.44×10^{1}	2.11×10^{1}	−0.5	3.78	6.07×10^{1}	3.12×10^{1}
−1.0	3.86	1.21×10^{2}	1.23×10^{2}	−0.5	3.86	2.51×10^{2}	1.63×10^{2}
−1.0	3.94	5.20×10^{2}	6.91×10^{2}	−0.5	3.94	7.51×10^{2}	7.69×10^{2}
−1.0	4.02	1.97×10^{3}	3.34×10^{3}	−0.5	4.02	1.79×10^{3}	3.36×10^{3}
−1.0	4.10	6.51×10^{3}	1.34×10^{4}	−0.5	4.10	5.15×10^{3}	1.37×10^{4}

The low temperatures coupled to the extremely large densities which characterize the atmospheres of objects with mass below 0.2 $M_\odot$ require a good non-ideal equation of state and a consistent treatment of opacities. Hence the physical environment where we expect our results to have the strongest impact is represented by the atmospheres of Population III very low-mass stars and brown dwarfs. The required extrapolations of the existing opacity tables (Cox & Tabor 1976; Stahler, Palla & Salpeter 1986) for $\rho > 10^{-3}$ g cm^{-3} prompted D' Antona (1987) to raise the question of the credibility of the existing theoretical models of such objects. More generally those opacity tables which are calculated ignoring all non-ideal effects in the optical properties of the matter have now been shown by Lenzuni, Chernoff & Salpeter (1991) to be unreliable in the regime of densities and temperatures relevant to the modeling of objects characterized by cold and dense atmospheres. Our new opacities where deviations from ideal behavior are accounted for, and extend to densities as high as 0.3 g cm^{-3}, represent at least a first step in the desired direction and should mitigate the concerns expressed in the literature. Qualitatively, the larger atmospheric opacities that we find imply lower values of the density at any given value of the optical depth in the atmosphere and marginally lower photospheric temperatures. We also expect the value of the minimum mass for hydrogen burning in Pop. III stars, previously estimated

at 0.115 $M_\odot$ (D' Antona 1987), to be moved downward closer to the value calculated for Pop. I stars (0.080–0.085 $M_\odot$, D'Antona & Mazzitelli 1985; Burrows, Hubbard & Lunine 1989). This prediction has been nicely confirmed by the recent results obtained by Saumon et al. (1992). In a preliminary set of evolutionary models of zero-metallicity brown dwarfs and low-mass stars, these authors find that the value for the minimum mass for hydrogen burning should indeed be revised to 0.094–0.098 $M_\odot$.

The sign of the effect is reversed in the limit where opacity is dominated by H^-. This is of specific interest for old, cool white dwarfs where diffusive settling of metals in the convection zone has probably operated to create extremely metal-poor atmospheres. The inclusion of non-ideal effects in the calculation of physical and optical properties of the H^- ion appears to give lower values of the Rosseland mean in the relevant regime of density and temperature than previously estimated (Cox & Tabor 1976). The implied photospheric densities and temperatures are larger that those predicted by the current models (D' Antona & Mazzitelli 1990). Again we want to stress that not only our calculation improves the quality of available opacities but it also extends the physical range over which these are calculated. Given the crucial dependence of cooling times of cool white dwarfs on the optical properties of the gas, our new opacities will likely have strong implications for the luminosity function of very old white dwarfs. In particular the predicted shortening of the cooling time scales is the opposite of what tentatively suggested by D' Antona & Mazzitelli (1989) as one of the possible explanations for the discrepancy between the observed and the theoretical luminosity function.

REFERENCES

Bouanich, J. P., Brodbeck, C., Van-Than, N., and Drossart, P. 1990, *J. Q. S. R. T.*, **44**, 393
Burrows, A., Hubbard, W. B., and Lunine, J. I. 1989, *Ap. J.*, **345**, 939
Chandra, S., Gaur, V. P., and Pande, M. C. 1991, *J. Q. S. R. T.*, **45**, 57
Chisholm, D. A., and Welsh, H. L. 1954, *Can. J. Phys.*, **32**, 291
Cox, A. N., and Tabor, J. E. 1976, *Ap. J. Suppl.*, **31**, 271
D' Antona, F. 1987, *Ap. J.*, **320**, 653
D' Antona, F., and Mazzitelli, I. 1985, *Ap. J.*, **296**, 502
D' Antona, F., and Mazzitelli, I. 1989, *Ap. J.*, **347**, 934
D' Antona, F., and Mazzitelli, I. 1990, *Ann. Rev. Astr. Ap.*, **28**, 139
Dossou, S., Clermontel, D., and Vu H. 1986, *Physica*, **139 & 140 B**, 541
Fontaine, G., Graboske, H. C, and Van Horn, H. M. 1977, *Ap. J. Suppl.*, **35**, 293
Hare, W. F. J., and Welsh, H. L. 1958, *Can. J. Phys.*, **36**, 88
Huber, K. P., and Herzberg, G. 1979, *Molecular Spectra and Molecular Structure. IV. Constants of Diatomic Molecules*, (Princeton, Van Nostrand)
Hummer, D. G., and Mihalas, D. 1988, *Ap. J.*, **331**, 794
John, T. L. 1988, *Astr. Ap.*, **193**, 189
Lenzuni, P., Chernoff, D. F., and Salpeter, E. E. 1991, *Ap. J. Suppl.*, **76**, 759
Lenzuni, P., Saumon, D., Van Horn, H. M., and Chernoff, D. F. 1992, in preparation
Magni, G., and Mazzitelli, I. 1979, *Astr. Ap.*, **72**, 134
Marley, M.S., and Hubbard, W. B. 1988, *Icarus*, **73**, 536
Meyer, W., Frommhold, L., and Birnbaum, G. 1989, *Phys. Rev. A*, **39**, 2434
Pekeris, C. L. 1962, *Phys. Rev.*, **126**, 1470
Saumon, D. 1989, Ph.D. thesis, University of Rochester
Saumon, D., Burrows, A., Hubbard, W. B., Lunine, J. I. 1992, in *Seventh Cambridge Workshop on Cool Stars, Stellar Systems, and the Sun*, A.S.P. Conference Series, in press
Saumon, D., and Chabrier, G. 1989, *Phys. Rev. Lett.*, **62**, 2397
Saumon, D., and Chabrier, G. 1991, *Phys. Rev. A*, **44**, 5122
Stahler, S. W., Palla, F., and Salpeter, E. E. 1986, *Ap. J.* **302**, 590
Tarafdar, S. P., and Vardya, M. S. 1970, *J. Q. S. R. T.*, **10**, 789
Van Kranendonk, J. 1957, *Physica*, **23**, 825
Van Kranendonk, J. 1959, *Physica*, **25**, 337
Yukhnovskii, P. I. 1988, *Soviet Materials Science*, **24**, 256

Paolo Lenzuni: Istituto di Astronomia, Università di Firenze, Largo E. Fermi 5, 50125 Firenze, ITALY.
Didier Saumon: Lunar and Planetary Laboratory, University of Arizona, Tucson AZ 85721, U.S.A.